Proceedings of the 25th Annual International Conference of the IEEE EMBS
Cancun, Mexico • September 17-21, 2003

Automatic Segmentation of Scanning Electron Microscopy Images for Molecular Aggregation Profiling

Fabrício Ourique, Vinicius Licks, Ramiro Jordan, Marios Pattichis
Electrical and Computer Engineering Department
University of New Mexico
Albuquerque, New Mexico 87131
Email: fourique,vlicks,pattichis,rjordan@eece.unm.edu

Abstract— **Scanning Eletron Microscopy (SEM) imaging has made it possible to obtain accurate inferences about functional intra-cellular events by the indirect observation of cell surface receptors' aggregation. Such observations are made with the use of colloidal gold particles that bind to the surface of specific ligands that cross-link to the desired receptors. Since the reliability of statistical inference methods about intra-cellular activities based on the observation of the receptors depend on the quality of the data set in hand, we propose in this paper a method to automatically segment gold labels in SEM images. This method includes an automatic thresholding operation aiming at simultaneously minimizing probabilities of false alarm and missed detection errors. Morphological filtering is used to deal with the partial superposition cases of structures of interest and additional median filtering is used for noise reduction purposes. We validate the method against a set of manually processed images of rat basophilic leukemia cells and we present results for the automatic estimation of aggregation density.**

I. Introduction

It is now well known that the primary mechanism by which cells interact with their surrounding environment is the binding of extra cellular molecules (ligands) to specific cell surface molecules (receptors). Besides being responsible for normal homeostasis related cell functions, the ligand-receptor binding phenomenon also constitutes the entrance gateway to the cell for toxins and viruses such as the cholera, and HIV. Cancer and genetic defects may also alter the structure of specific receptors, deregulating functions such as growth control, and cholesterol processing [1].

Due to the diffusion of receptors in the cell surface, these structures can form aggregations such as those induced by the binding of ligands to the surface of two or more receptors. This phenomenon, named cross-linking, can launch a series of events that may lead to cell differentiation and proliferation, such as the formation of antibody secreting cells or the release of histamine from intracellular granules in certain types of allergic reactions. Therefore, due to the importance of the receptor aggregation phenomenon in functional cellular responses, it is possible to gain a detailed understanding of such processes by observing the associated movement and aggregation of receptors in the cell surface. In the past, inferences about the underlying mechanisms of such aggregations and interactions with intracellular activities have been based on indirect experimental evidence. Nowadays, scanning electron microscopy (SEM) makes it possible to directly observe diffusion/aggregation processes at the molecular level using colloidal gold molecule labels [2]. These colloidal gold particles adhere to the surface of receptor-bound ligands, thus allowing the labeling of such structures and subsequent analysis based on the properties of these aggregations (e.g. the mean aggregate size).

Such a quantitative analysis of SEM images significantly increases the relevance of using appropriate image segmentation pre-processing methods that will allow for the accurate labeling of regions of interest (ROI) that will constitute a reliable basis for the subsequent application of statistical inference methods.

This paper focuses on the implementation of a method for the automated segmentation of colloidal gold particles in SEM images. For that purpose, the test images were first pre-processed by an automatic thresholding technique to minimize the expected number of labeling errors. Then, morphological filtering was used prior to binary labeling in order to overcome the effect of partial superposition of the gold labels. Eventually, median filtering was used for speckle noise reduction purposes.

II. Obtaining cell data

The test images were obtained from Rat Basophilic Leukemia cells. These cells, with a homogeneous receptor distribution of IgE antibodies, were incubated with IgG antibodies ligand and further treated with fixative to avoid the diffusion and redistribution of the receptors during the data collection. Then, the cells were incubated with colloidal gold particles in order to label receptor-bound ligands [1]. The ESM images were photographed, digitized into images of 6728 by 5948 pixels, 16 bits gray-level representation and subsequently stored into TIFF raw format.

For the experiment in hand, we assume that an aggregation is represented by a set of gold labels that are contained in a higher dimensional set of receptors (cell-bound antibodies),

0-7803-7789-3/03/$17.00 ©2003 IEEE

ligands (antibodies in solution) and colloidal gold particles. Thus, we should emphasize that the number of gold particles in an aggregation will not be necessarily equal to the number of receptors in the same region of interest. This fact is due to eventual imperfections in the gold label incubation processes and should be taken into account when making inferences about the ligands based on the statistics of the aggregates. We shall not be concerned with such a problem in this paper, since we are only interested in the reliable automated segmentation of given test images, with no concern to the process used to obtain them.

III. Methodology

As we mentioned previously, the SEM collected image was digitized into an 6728 by 5948 pixel image. In order to validate the proposed segmentation method, we divided this image in 20 partitions of 1024 by 1024 pixels. Figure 1 shows one such partition. Gold labels are depicted as the darker regions. Observe the overlapping effect produced by the superimposed labels. From these segments, we obtained the ground-truth, which consisted in the manual segmentation of all the gold labels and background pixels followed by the quantification of the aggregates' size present in each sub-image. The ground-truth data is presented in Table I. Furthermore, half of the ground-truth data set was used to obtain estimates of the probability density functions (PDFs) of the gold labels $f_S(s)$ and of the background pixels $f_B(b)$ based on their respective pixel intensity histograms.

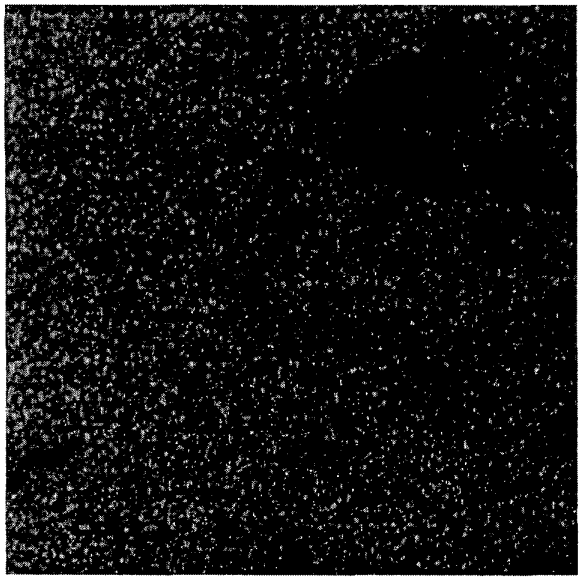

Fig. 1. Partition of The Original Image

A. Automated thresholding

During the thresholding process, a pixel that belongs to the background can be erroneously classified as a gold label and in the same fashion, a gold label pixel can be classified as a background pixel. These two classification mistakes are named False Alarm (FA) and Missed-Detection (MD) errors, respectively. Furthermore, we can define the probability of occurrence of these errors as:

$$P_{MD} = \int_{\tau}^{\infty} f_S(s)ds \tag{1}$$

$$P_{FA} = \int_{0}^{\tau} f_B(b)db \tag{2}$$

where τ is the threshold. In order to simultaneously minimize P_{MD} and P_{FA}, an optimal threshold $\tau^\star$ has to be assigned. This optimal threshold can be automatically found using a simple bisection search strategy over the whole range of possible values of τ. For each value of τ, the image is thresholded and P_{MD} and P_{FA} are evaluated using the ground-truth information. The process is repeated until $P_{MD} = P_{FA}$, when $\tau = \tau^\star$. This search is undertaken on the training set partition of the ground-truth, which accounts for half of the whole data set. Finally, the image is thresholded by $\tau^\star$ such that:

$$I_{th}(x,y) = \begin{cases} 0 & \text{if } I(x,y) < \tau^\star, \\ 1 & \text{otherwise} \end{cases} \tag{3}$$

where $I(x,y)$ is the original image, and $I_{th}(x,y)$ is the result of the threshold operation with $\tau^\star$ that minimizes simultaneously the false alarm and the missed-detection probabilities.

B. Filtering

After thresholding, the image partitions were subjected to a median filtering operation on a 5x5 kernel. This filtering operation was intended to eliminate remaining noise inclusions that clearly were not part of the gold labels due to their comparatively reduced dimensions. The size of the median filter kernel was chosen empirically based on the observation that isolated points which did not connect into a 5x5 region were unlikely to belong to a gold label structure.

Since the images at hand were the result of the projection of three-dimensional structures on a two-dimensional plane, it was likely that two or more gold labels would overlap in the resulting projection, thus forming only one individual connected set. Since these imperfections could affect subsequent inferences about the aggregations based on the cardinality of the segmented set of connected regions, this problem had to be overcome. This was accomplished by the use of a binary morphological opening filter. Let $\tilde{I}_{th}$ be the result of optimally thresholding the original image and subsequentelly passing it through a medium filter. Let B be the structuring morphological element given by:

$$B = \begin{bmatrix} 0 & 1 & 0 \\ 1 & 1 & 1 \\ 0 & 1 & 0 \end{bmatrix} \tag{4}$$

The result of passing $\tilde{I}_{th}$ through the opening filter resulting in F is represented below as

$$\begin{aligned} F &= \tilde{I}_{th} \circ B \\ &= (\tilde{I}_{th} \ominus B) \oplus B \end{aligned} \tag{5}$$

where $\circ$, $\ominus$ and $\oplus$ represent the opening, erosion and dilation binary morphological operators, respectively.

C. Labeling

Finally, the morphologically filtered image F was submitted to a binary labeling operation in order to segment and to identify each individual gold particle. The labeling operation assigns a unique pixel value to different connected regions. In this paper, connectivity is defined over a 4-neighborhood and based on the condition that connected pixels have luminance values equal to 0. This allows us to know the number of connected regions and their relative areas with a simple inspection of the labeled image's histogram.

IV. Results

Figure 2 illustrates the assignment of the optimal threshold τ^* as a function of the false alarm and missed detection probability curves. Note that τ^* is assigned to be at the intersection of these curves, which guarantee that both probabilities of error will be simultaneously minimized. The method to find the optimal threshold value was described in detail in section III-A. Obviously, alternative cost functions could be used in the minimization problem, such as the average probability of classification error, for example.

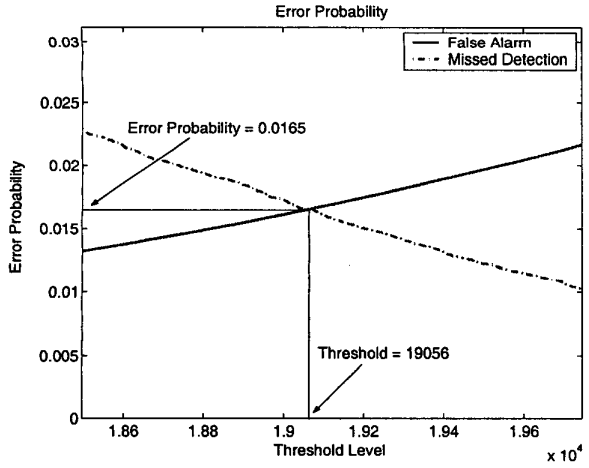

Fig. 2. Assignment of the optimal threshold value τ^*

Figure 3 shows a plot of Sensitivity versus false alarm probability for different values of the threshold level, as indicated. Sensitivity and Specificity are defined as $(1-P_{MD})$ and $(1-P_{FA})$, respectively. Note that around τ^* (i.e. $\tau = 19,056$), small changes in the threshold level cause large variations of the error probabilities.

Finally, Table I presents a quantitative view of the results found. Observe that the amount of gold labels and their

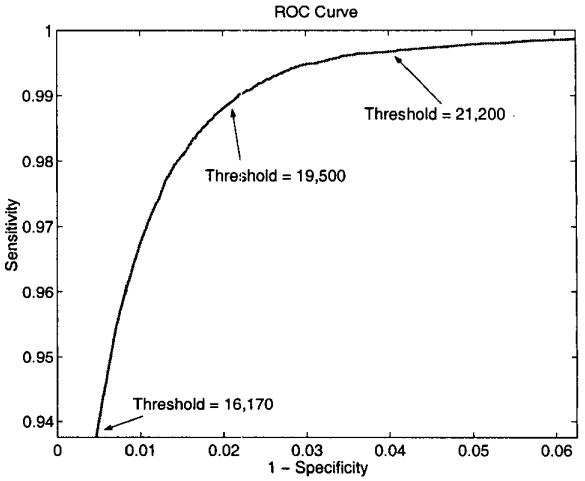

Fig. 3. Sensitivity and specificity graphs as functions of the threshold

respective relative areas were accurately estimated by the automated segmentation technique devised in this paper. The only exception found was on Partition #8, where there was a relatively high error rate in the estimated number of gold labels. As it can be seen in Figure 4, the presence of artifacts attributed to a non-homogeneous distribution of the fixative has biased the automated segmentation algorithm to detect gold labels where there were none.

Image Partitions	Ground-truth		Estimation	
	Area	# of Gold Particles	Area	# of Gold Particles
Partition # 1	0	0	0	0
Partition # 2	0	0	0	0
Partition # 3	0	0	0	0
Partition # 4	0	0	0	0
Partition # 5	6,446	10	6,615	10
Partition # 6	7,384	10	8,340	7
Partition # 7	0	0	0	0
Partition # 8	4,293	6	4,658	10
Partition # 9	2,752	4	2,677	4
Partition # 10	1,922	4	2,777	4
Partition # 11	566	1	611	2
Partition # 12	5,874	4	3,167	5
Partition # 13	0	0	0	0
Partition # 14	0	0	0	0
Partition # 15	0	0	0	0
Partition # 16	2,635	4	2,348	4
Partition # 17	6,118	8	5,566	8
Partition # 18	2,132	4	2,447	4
Partition # 19	5,454	8	5,477	8
Partition # 20	535	1	399	1
Total	46,111	64	46,278	67

TABLE I
AREAS OF GOLD-PARTICLES ESTIMATED

V. Conclusions

In this paper we addressed the problem of automatically segmenting SEM images for use in molecular aggregation profiling. The issues of speckle noise contamination and

partially overlapping labels were overcome with the use of a binary median filter followed by a morphological opening operator. The optimal threshold level was automatically assigned using an iterative bisection search procedure aiming at simultaneously minimizing the probabilities of false alarm and missed detection. This threshold assignment procedure was done using training data consisting on half of the whole data set. Finally, the proposed method was validated by direct comparison of the results found with a manually generated ground truth.

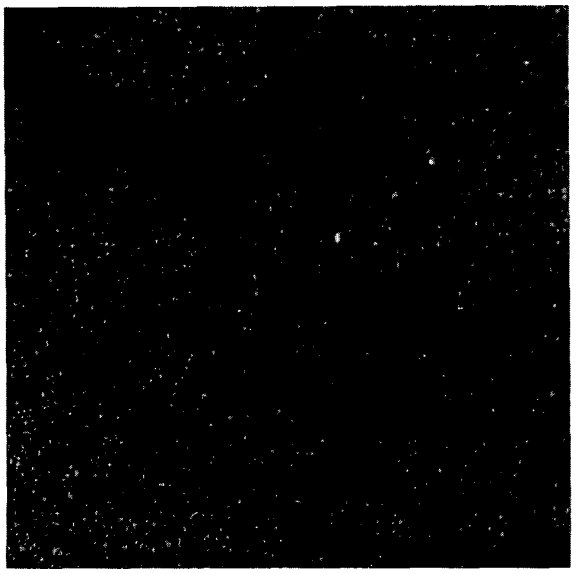

Fig. 4. Image of Partition #8

VI. Acknowledgements

The authors would like to thanks to Dr. Janet M. Oliver, who kindly supplied the images of Rat Basophilic Leukemia cells used in this paper. Dr. Oliver is with the School of Medicine, Cell Pathology Laboratory at the University of New Mexico.

References

[1] Margaret L. Sanders, Janet M. Oliver, Gregory W. Donohoe, Matthew J. Pujol, and Carla Wofsy, "Characterizing Molecular Aggregation on Cell surfaces from Spatial Point Patterns," Technical Report - School of Medicine - The University of New Mexico, 1997.

[2] G.M. Hodges, "On the Molecular Profiling of Cell Surfaces by SEM," *Arch. Histol, Cytol.*, , no. 55, pp. 27–38, 1992.

[3] F. Schonorrenberg, C.S. Pattichis, C.N. Schizas, K. Kyriacou, "Content-Based Retrieval of Breast Cancer Biopsy Slides," Technical Report - Department of Electron Microscopy - The Cyprus Institute of Neurology and Genetics , 2002.

[4] Bridget Wilson, Janet Pfeiffer, Zurab Survilad, Elizabeth Gaudet, Janet Oliver, "High resolution mapping of mast cell membranes reveals primary and secondary domains of $Fc\epsilon RI$ and LAT," August 2001.

[5] Rafael Gonzalez, Richard Woods, *Digital Image Processing*, Prentice Hall, 2002.